2_C49

# Numerical Analysis on the Applicability of Air Purifier for Removal of Indoor Viral Contaminants

**Yunchen Bu**

**Ryozo Ooka, PhD**
*Member ASHRAE*

**Hideki Kikumoto, PhD**
*Member ASHRAE*

**Wonseok Oh, PhD**

## ABSTRACT

*Many recent studies have been reported that the novel coronavirus (SARS-CoV-2) can spread through an airborne transmission route. Although ventilation is generally adopted to control viral infection through airborne transmission, a high ventilation rate will increase the energy consumption of air conditioning. Under such condition, the portable HEPA-filter air purifier might be an effective supplementary measure. However, past discussions on its efficacy in reducing indoor infection risks are limited. Therefore, this study aims to conduct a systematic investigation on the applicability of air purifier using Computational Fluid Dynamics (CFD) simulation. Two scenarios both with an air change rate of 0.5 1/h were considered. In Scenario a, a general room with size being 4 m × 5 m × 2.5 m (13.1 ft × 16.4 ft × 8.2 ft) was adopted. Viral contaminants were set as homogeneous emission. In Scenario b, a 6-mat bedroom with size being 2.7 m × 3.6 m × 2.5 m (8.9 ft × 11.8 ft × 8.2 ft) was adopted. Viral contaminants were assumed to be generated from a lying infector at 27 quanta/h constantly. The purifier was operated at a flow rate of 90 $m^3$/h (3178 $ft^3$/h). The results showed that a general household HEPA-filter air purifier has high effectiveness in removing indoor viral contaminants and infection risks. In Scenario b, to reach an infection probability of 0.2, it took a susceptible person only about 10 min of exposure time without purifier, but up to 50 min with a purifier. A larger flow rate can contribute to higher purifying effectiveness and a more thorough air mixing indoor. Moreover, the purifying effectiveness, distribution of contaminant concentration and infection probability were found to be influenced by the relative positions of the purifier inlet and outlet, ventilation air supply and exhaust, virus generation source, and indoor obstacles.*

## INTRODUCTION

The global spread of coronavirus disease 2019 (COVID-19) has posed a significant threat to human health, making it urgent to seek out efficient infection control methods. Existing evidences strongly indicate that the novel coronavirus (SARS-CoV-2) could spread through the airborne transmission route (Morawska and Cao 2020; Yao et al. 2020). Among control strategies against viral infection through airborne transmission, ventilation is most generally adopted, by introducing outside air to reduce indoor virus concentration. However, from the perspective of heating and cooling loads, it is difficult to increase the ventilation rate without limit for energy saving, which calls for other possible solutions. The portable air purifier, especially those with high-efficiency particulate air (HEPA) filters, could be a potential supplementary measure (Zhao, Liu, and Chen 2020).

Concerning the cleaning performance of the portable HEPA-filter air purifier, the single pass efficiency for particle filtration could be up to 99.97% (Kowalski, Bahnfleth, and Whittam 1999). Compared with other common purifying technologies, the HEPA filter was examined to be among the most effective types on removing size-resolved influenza particles due to coughing and sneezing (Zuraimi, Nilsson, and Magee 2011). As for a typical ward with a size of 109 $m^3$ (3849.3 $ft^3$), a common portable HEPA-filter purifier could reach an effective air change rate from 2.7 to 5.6 1/h (Qian et al. 2010). HEPA-filter purifiers are also featured with strong outlet momentum. It was found to produce global air mixing indoor at high speed (Qian et al. 2010). Moreover, flow interaction between other momentum sources (e.g. ventilation systems) and purifiers could greatly influence indoor air purifying effectiveness. Therefore the parameters and positioning coordination of momentum sources should assure a well-organized air circulation (Zhang et al. 2010). On the other hand, considering the characteristics of contaminants, it was found that when airborne particles are distributed uniformly in the room, the flow rate of the purifier affects the concentration most, while the purifier position plays a role at low flow rates (Jin et al. 2016).On the other hand, under non-uniform aerosol distributions caused by smoking or coughing, the purifier position affects the concentration most, while the expiratory airflow velocity and the purifier orientation also plays a role (Chen et al. 2017).

From previous studies, we could conclude that factors which affect the air purifier effectiveness in removing indoor viral particles and concentration distribution include contaminant sources, sinks and airflow interaction. However past discussions are limited in fully considering the relationship of these factors from a systematic perspective. Additionally, compared to experiments that could only measure limited points of concentration and take a long time, CFD simulation could provide detailed information of the fluid and concentration field for the whole calculation domain, as well as evaluate different cases by modifying boundary conditions conveniently. Therefore, a systematic investigation of air purifier efficacy in removing indoor viral contaminants and infection risks was conducted here using the CFD simulation.

This research considers two scenarios. Firstly in an empty room, we will investigate how different flow rates and layouts of the purifier influence its overall purifying effectiveness and concentration distribution of viral contaminants. Viral contaminants are assumed to be homogeneously generated in the whole room, since generally the contaminant source position is hard to determine. Secondly, we will investigate the effect of the purifier on reducing infection risks caused by a mildly ill or asymptomatic COVID-19 patient lying in a typical Japanese 6-mat bedroom, which represents the general scenario of self-isolation in hotel or at home.

## METHODOLOGY

### Numerical analysis on concentration of viral contaminants under homogeneous emission

**Simulation outline.** For Scenario a, as shown in Figure 1(a), the portable HEPA-filter air purifier was placed in a typical room with a size of 4 m × 5 m × 2.5 m (13.1 ft × 16.4 ft × 8.2 ft). The air change rate (ACH) for the room ventilation was set 0.5 1/h (Table 2) constantly, which is mandatory in Japanese houses. The applicability of the air purifier with different parametric settings is the focus of this study, and the ventilation only functions to ensure certain fresh air supply. The simulated portable HEPA-filter air purifier refers to parameters of general household types sold in Japan, simplified as a 0.40 m × 0.24 m × 0.64 m (1.31 ft × 0.79 ft × 2.10 ft) block. The ventilation supply, ventilation exhaust, purifier inlet and purifier outlet are recorded as Inlet 1, Outlet 1, Outlet 2 and Inlet 2 respectively, indicating their flow direction relative to the calculation area. The air purifier inlet has the same flow rate as the outlet. The velocity of air purifier inlet and outlet is calculated according to the flow rate of each simulation case. The single pass efficiency of the HEPA-filter was set 99.97% (Kowalski, Bahnfleth, and Whittam 1999), therefore the contaminant mean concentration (C) on the purifier outlet (Inlet 2) was set to be 0.03% of that on the purifier inlet (Outlet 2). The viral contaminants were set as homogeneous emission, that the emission rate was 1/s equally in all parts of the room. The viral contaminants causing the airborne infection were represented by passive scalars, which do not affect the velocity field of the ambient airflow and do not consider gravitational settlement or deposition on wall. Other calculation conditions are shown in Table 1.

Table 2 shows simulation cases. Five different positions and two orientations (Figure 2(a)) of the air purifier, as well as three different flow rates being 100, 200 and 400 $m^3/h$ (3531, 7063 and 14126 $ft^3/h$) are considered. ‘Front’ means the purifier inlet is facing the ventilation supply, and ‘Back’ means the purifier inlet is back to the ventilation supply. Case a-0, a-1, a-6 and a-7 are proposed to examine the influence of different flow rates, with Case a-0 (no air purifier) serving as a reference case. Case a-1, a-2, a-3, a-4, a-5F and a-5B are designed to study the influence of different positions and orientations.

The commercial CFD software Star-CCM+ (Ver. 14.06) was employed in this study. The Reynolds Averaged Navier Stokes (RANS) equations with Low Reynolds number k-ε model (F.S. Lien et al 1996) were used for turbulence modeling, and the SIMPLE method was used for calculation algorithm. For both velocity and scalar, the convection terms were discretized using the second-order upwind scheme, while the diffusion terms were discretized using the second-order central scheme. The velocity and concentration fields of the indoor flow were calculated under steady state condition. Trimmed Cell and Prism Layer were set for mesh division. The total number of spatial grids was around 750,000 cells for the case without air purifier, and around 2,000,000 cells for cases with air purifier.

## Numerical analysis on infection risk with infector lying in bedroom

**Simulation outline.** In Scenario b (Figure 1(b)), a 6-mat Japanese bedroom with size being 2.7 m × 3.6 m × 2.5 m (8.9 ft × 11.8 ft × 8.2 ft) was considered. Here 6-mat is the standard size for a one-person Japanese bedroom, and one mat is about the size of 0.9 m × 1.8 m (3.0 ft × 5.9 ft). A bed is placed in the center of the room against a wall, and an infector was assumed to be lying on the bed. As shown in Table 1, the room air change rate was assumed to be 0.5 1/h as well. From the ventilation supply, the air flowed horizontally at 20 °C (68.0 °F), at a speed of 0.075 m/s (0.246 ft/s). The purifier applied in this scenario also has a single pass efficiency of 99.97%, but a constant airflow rate of 90 $m^3$/h (3178 $ft^3$/h) targeting at a 6-mat room. The viral contaminants were assumed to be generated by nasal breathing of the infector in the unit of quanta, which refers to the number of infectious airborne particles required to infect a person (Wells 1955). Since the majority of exhaled particles are less than 1 μm ($4 \times 10^{-5}$ inch) in diameter, which can suspend in the air as aerosols for long time and distances (Fabian et al. 2008), and viruses are considered to be attached to expiratory aerosols (Qian et al. 2009), the quanta in this study were assumed as passive scalar as well. The amount of quanta generated per infector varies from study to study, and there is no definite value by far. Therefore in this study, the calculation method from Kriegel et al. was temporarily used to obtain a virus generation rate of about 27 quanta/h while breathing at rest (Kriegel et al. 2020). Other calculation conditions are shown in Table 1.

Simulation cases are shown in Table 2. Three locations (Figure 2(b)) with or without an air purifier were considered.

CFD simulation setups are basically the same as Scenario a. Exceptionally, Realizable k-ε model was used for turbulence modeling (Zhai et al. 2007). In addition, Boussinesq approximation were used for buoyancy force. Only convection calculations were performed without considering radiation. Polyhedral Cell and Prism Layer were set for mesh division. The total number of spatial grids was around 280,000 cells for the case without air purifier, and around 400,000 cells for cases with air purifier.

**Assessment of local airborne infection risk.** In this study, we quantitatively evaluated airborne infection risk due to the breathing of the infector and susceptible person using the Wells-Riley model shown in Equation (1) (Wells 1955; Riley, C.E., Murphy, G. and Riley 1978).

$$P_I = 1 - e^{-\frac{I\,q\,p\,t}{Q}} \quad (1)$$

Where $P_I$ is the probability of infection, $I$ is the number of infectors, $q$ is the quanta generation rate by one infector (quanta/h), $p$ is the breathing rate of each susceptible person ($m^3$/h or $ft^3$/h), $t$ is the exposure time interval (h), and $Q$ is the room ventilation rate ($m^3$/h or $ft^3$/h). Originally, the Wells-Riley model assumed a uniform quanta concentration in the whole space, without considering the quanta concentration distribution. To predict the distribution of infection probability in the breathing zone, the Wells-Riley model and the quanta concentration distribution calculated by CFD were integrated, and the local airborne infection risk was evaluated by Equation (2) (Qian et al. 2009).

$$P_I = 1 - e^{-p\,C_{q,i}\,t} \quad (2)$$

Where $C_{q,i}$ is the quanta concentration in the breathing zone of the susceptible person (quanta/$m^3$ or quanta/ $ft^3$). $i$ is the spatial location of a point in the breathing zone. Here, $p$ was taken to be 0.54 $m^3$/h (19.07 $ft^3$/h) (for low activity: sitting and standing) (Kriegel et al. 2020). Additionally, if protection effects of masks from both the infector and susceptible person were considered as well (Dai and Zhao 2020), Equation (2) can be further transferred into Equation (3) by incorporating the mask filtration efficiency.

$$P_I = 1 - e^{-(1-\eta_I)(1-\eta_S)p\,C_{q,i}\,t} \quad (3)$$

Where $\eta_I$ is the filtration efficiency of the infector's mask, $\eta_S$ is the filtration efficiency of the susceptible's mask. Here,

the filtration efficiency of surgical masks was set as 44% for $\eta_I$ (at rest) and 10% for $\eta_S$ (in moderate activity), if considering the influence of air leakage through the mask fitting gap (Konda et al. 2020).

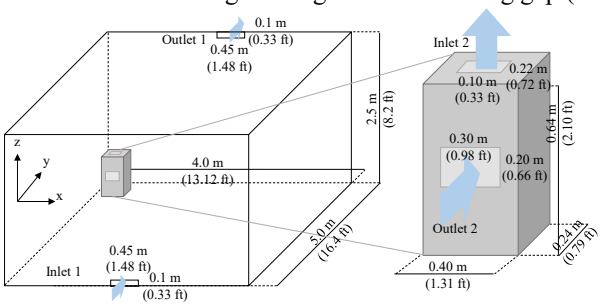


(a) Scenario a

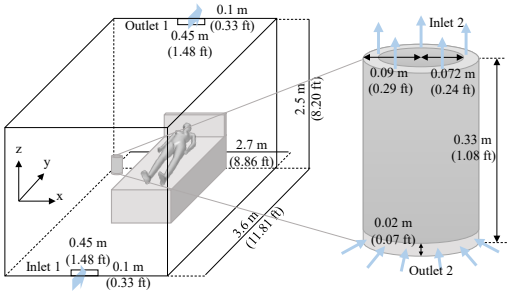


(b) Scenario b

**Figure 1** System geometry and simulation geometry

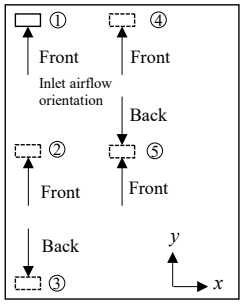


(a) Scenario a

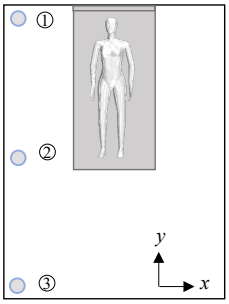


(b) Scenario b

**Figure 2** Layout of the air purifier

**Table 1. Numerical analysis and boundary conditions**

| Item | | Scenario a | Scenario b |
|---|---|---|---|
| Ventilation | Supply (Inlet 1) | ACH = 0.5, v = 0.155 m/s (0.509 ft/s)<br>Turbulent intensity = 5%,<br>Length scale = 0.07 · $L$ m (0.23 · $L$ ft) | ACH = 0.5, v = 0.075 m/s (0.246 ft/s)<br>Turbulent intensity = 5%,<br>Length scale = 0.07 · $L$ m (0.23 · $L$ ft) |
| | Exhaust (Outlet 1) | Static pressure $P$ = 0 Pa | Based on the law of conservation of mass |
| Air purifier | Inlet (Outlet 2) | Size: 0.30 (x) m × 0.20 (z) m (0.98 ft × 0.66 ft),<br>Flow rate: 400, 200, 100 m$^3$/h (14126,7063,3531 ft$^3$/h),<br>v = 1.85, 0.93, 0.46 m/s (6.07, 3.05, 1.51 ft/s)<br>Turbulent intensity = 5%,<br>Length scale = 0.07 · $L$ m (0.23 · $L$ ft) | Size: 0.57 m × 0.02 m (1.87 ft × 0.07 ft),<br>Flow rate: 90 m$^3$/h (3178 ft$^3$/h),<br>v = 1.50 m/s (4.92 ft/s)<br>Turbulent intensity = 5%,<br>Length scale = 0.07 · $L$ m (0.23 · $L$ ft) |
| | Outlet (Inlet 2) | Size: 0.22 (x) m × 0.10 (y) m (0.72 ft × 0.33 ft)<br>Flow rate: 400, 200, 100 m$^3$/h (14126,7063,3531 ft$^3$/h),<br>v = 5.05. 2.53, 1.26 m/s (16.57, 8.30, 4.13 ft/s)<br>Turbulent intensity = 5%,<br>Length scale = 0.07 · $L$ m (0.23 · $L$ ft)<br>Concentration: C (Inlet 2) = C (Outlet 2) × 0.03% | Area: 8.98 × 10$^{-3}$ m$^2$ (96.66 × 10$^{-3}$ ft$^2$),<br>Flow rate: 90 m$^3$/h (3178 ft$^3$/h),<br>v = 2.78 m/s (9.12 ft/s),<br>Temperature: the same as Outlet 2<br>Turbulent intensity = 5%,<br>Length scale = 0.07 · $L$ m (0.23 · $L$ ft)<br>Concentration: C (Inlet 2) = C (Outlet 2) × 0.03 % |
| Wall | | No-slip, heat insulation | No-slip, heat insulation |
| Human | Size | No human,<br>Contaminant source: homogeneous emission,<br>Contaminant emission rate: 1 [1/s] | Height: 1.65 m (5.41 ft),<br>Surface area in contact with air: 1.11 m$^2$ (11.95 ft$^2$) |
| | Surface | | No-slip,<br>Convection heat transfer coefficient: 23 W/m$^2$ (0.002 Btu/s · ft$^2$) (Zhu, Kato, and Yang 2006) |
| | Nose | | Velocity: No; Quanta emission rate: 27 quanta/h (Kriegel et al. 2020) |

**Table 2. Simulation cases**

| Case number | Position of the air purifier | Orientation of inlet airflow | Airflow rate [$m^3/h$] ([$ft^3/h$]) |
|---|---|---|---|
| Case a-0 | No air purifier | - | - |
| Case a-1 | Scenario a-① | Front | 400 (14126) |
| Case a-2 | Scenario a-② | Front | 400 (14126) |
| Case a-3 | Scenario a-③ | Back | 400 (14126) |
| Case a-4 | Scenario a-④ | Front | 400 (14126) |
| Case a-5F | Scenario a-⑤ | Front | 400 (14126) |
| Case a-5B | Scenario a-⑤ | Back | 400 (14126) |
| Case a-6 | Scenario a-① | Front | 100 (3531) |
| Case a-7 | Scenario a-① | Front | 200 (7063) |
| Case b-0 | No air purifier | - | 90 (3178) |
| Case b-1 | Scenario b-① | - | 90 (3178) |
| Case b-2 | Scenario b-② | - | 90 (3178) |
| Case b-3 | Scenario b-③ | - | 90 (3178) |

## RESULTS AND DISCUSSION

### Influence on viral contaminant concentration under homogeneous emission

**Influence of air purifier flow rate.** Figure 3 shows the volume mean concentration and ventilation exhaust mean concentration under cases with different flow rates. The ventilation exhaust mean concentration of Case a-0 (no air purifier) were used as a benchmark concentration when calculating relative concentration. Both concentration indicators dramatically decreased in Case a-6 (100 $m^3/h$), a-7 (200 $m^3/h$) and a-1 (400 $m^3/h$) compared with that in Case a-0 (no air purifier). The volume mean concentration with the flow rate being 100, 200 and 400 $m^3/h$ (3531, 7063 and 14126 $ft^3/h$) can be reduced to 1/5, 1/10 and 1/18 of that with no air purifier indoor respectively. This shows that a general household HEPA-filter air purifier can significantly reduce the concentration of indoor viral contaminants. The larger the flow rate is, the higher overall purifying effectiveness could be. However, the purifying effectiveness will increase more slowly when the flow rate becomes larger. Moreover, larger flow rates may lead to noise and draft problems when the air purifier is not appropriately designed. For example, the operation sound for the 400 $m^3/h$ level of the air purifier we referred to can be about 55dB, which might not be qualified for some living scenarios.

Figure 4 shows the relative concentration distribution of viral contaminants at different heights when set with different flow rates. z = 0.1 m (0.32 ft) and z = 2.4 m (7.87 ft) represent the height of ventilation supply and exhaust respectively, while z = 1.1 m (3.61 ft) represents the height of breathing zone when sitting. For all height levels, when the flow rate became larger, not only the concentration decreased, the airflow pattern created by the ventilation and purifier also became more indistinct. This shows that a stronger airflow from the purifier could create a more complete indoor air mixing.

**Influence of air purifier position and orientation.** Figure 5 shows the volume mean concentration and mean concentration of ventilation exhaust under cases with different positions and orientations. The flow rate was set 400 $m^3/h$ (14126 $ft^3/h$) for all cases. The mean concentration of Case a-1, a-2 and a-3 displayed an increasing trend, and the mean concentration of Case a-5B was lower than that of Case a-5F. It shows that when the purifier inlet was further away from the ventilation supply, the overall purifying effectiveness would become higher. This is because the air purifier will dispose more contaminated air rather than the clean air provided from the ventilation supply. Moreover, the mean concentration on ventilation exhaust of Case a-4 was much lower than other cases. It shows that when the purifier outlet is close to the ventilation exhaust, air exhausted from the ventilation exhaust is mainly the purified air from the purifier. However, there were no significant differences between the volume mean concentration of Case a-4 and other cases, showing that the contaminant amount exhausted from ventilation exhaust has little influence on the overall purifying effectiveness. This is because the flow rate of the air purifier (400 $m^3/h$ or 14126 $ft^3/h$) is much larger than that of the ventilation (25 $m^3/h$ or 883 $ft^3/h$), making the air purifier contribute to the purification mostly.

Figure 6 shows the mean concentration distribution of viral contaminants when set with different positions and orientations. When z = 0.1 m (0.32 ft), the concentration was extremely low closed to the ventilation supply, but the concentration field soon merged a short distance away. By contrast, when z = 2.4 m (7.87 ft), the space right above the air

purifier's outlet still shows extremely high concentration, indicating that the airflow from the air purifier is much stronger than that from the ventilation. When z = 1.1 m (3.61 ft), two parts with relatively higher concentration could be seen in different cases. This shows that each case has relatively more dangerous zones to sit in. The position of the more dangerous zones depends on the position and orientation of the air purifier.

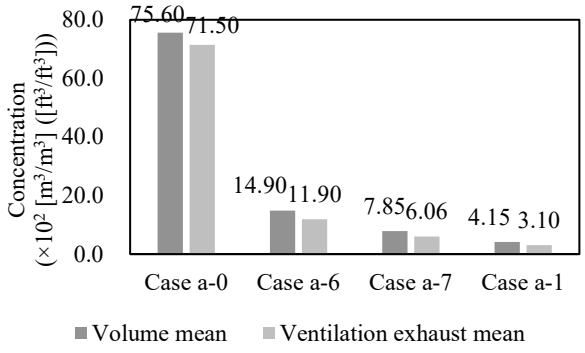


**Figure 3** Contaminant concentration under different airflow rates

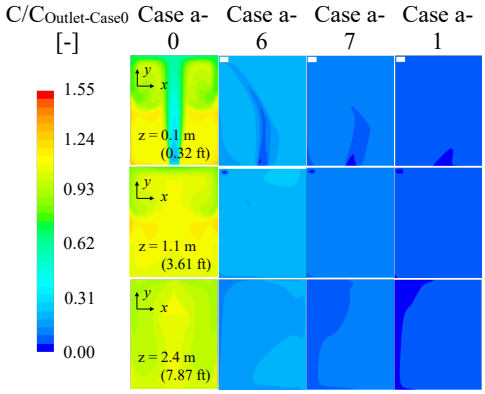


**Figure 4** Relative concentration ($C/C_{Outlet\text{-}Case0}$) distribution under different airflow rates

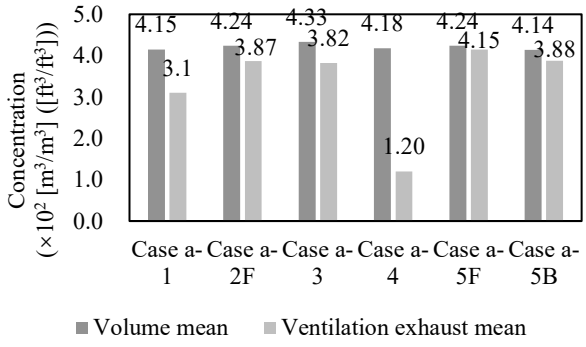


**Figure 5** Contaminant concentration under different layouts

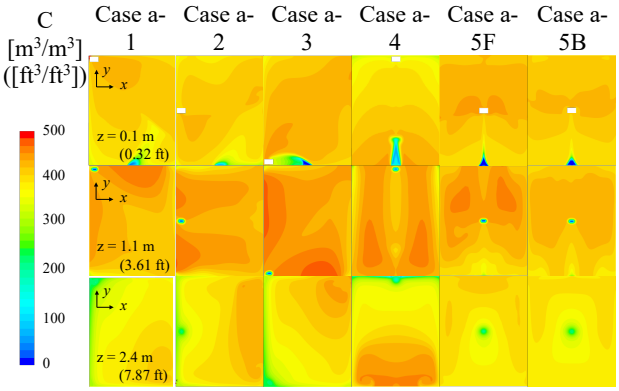


**Figure 6** Concentration (C) distribution under different layouts

## Influence on infection risk with infector lying in bedroom

The results of horizontal planes with height of 1.1 m (3.61 ft) and 1.5 m (4.92 ft) were analyzed, referring to the height of human's breathing zone when sitting and standing respectively.

**Influence of air purifier availability, mask wear and exposure time.** The mean infection probability as a function of exposure time for each case when z = 1.5 m (4.92 ft) is shown in Figure 7(a). The infection probability in Case b-0 without an air purifier increases quickly, and already exceeds 0.2 at 10 min after the susceptible person enters the room. On the other hand, the infection probability in Case b-1, Case b-2 and Case b-3 (the cases with the air purifier set at different locations) increases linearly with time and more slowly than in Case b-0 (the case without an air purifier), reaching 0.2 at about 50 min after entrance. Therefore, when staying in a 6-mat room with a lying infector, the risk of airborne infection can be greatly reduced when an air purifier with 90 $m^3/h$ (3178 $ft^3/h$) airflow rate is introduced, compared to the situation that no air purifier is introduced.

In addition, if both infector and susceptible person wear a surgical mask, the mean infection probability can be further reduced in all cases, as shown in Figure 7(b). Infection risks in cases with purifier can be reduced to almost half of the original.

**Influence of air purifier position.** Though Figure 7(a) shows that the mean infection probability when z = 1.5 m (4.92 ft) does not differ much depending on the air purifier position, the mean infection probability in Case b-1 is slightly higher.

Figure 8 shows the infection risk distribution in each case when the exposure time reaches 0.5 h. Case b-1 also has a larger area of high risk than Case b-2 and b-3. Considering this, there might be two causes: one is that the purifier in Case b-1 has difficulty in removing the blocked viral contaminants on the right side of the bed; the other is that the airflow of the purifier in Case b-1 is close to the ventilation exhaust, thus part of the purified air is directly discharged.

On the other hand, as shown in Figure 8, for all cases the infection risk when z = 1.5 m (4.92 ft) diffuses more than that when z = 1.1 m (3.61 ft). In Case b-2 and Case b-3, the peak points of infection probability also gravitate toward the purifier as the height increases. This may be due to the fact that the purifier is at some distance from the virus source and the ventilation exhaust, and the height of the purifier is lower than that of the virus source. Since the purifier is farther away from the virus source in Case b-3, the infection risk spreads more widely as well.

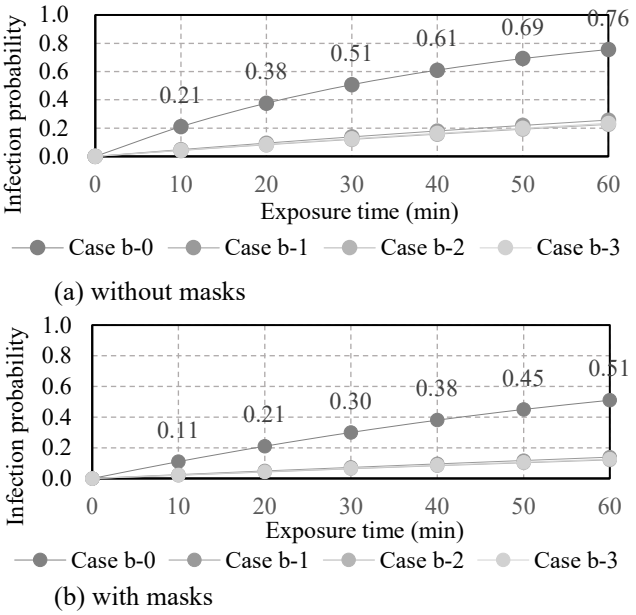


**Figure 7** The relationship between mean infection probability and exposure time of each case

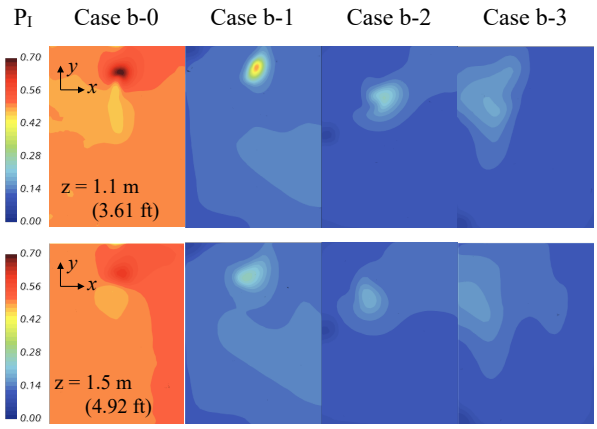


**Figure 8** Infection probability distribution on z = 1.1 m (3.61 ft) and z = 1.5 m (4.92 ft) (exposure time = 0.5 h)

## CONCLUSION

In this study, the applicability of air purifier and mask wearing in removing indoor viral contaminants and infection risks were examined to provide guidance on infection control measures when it is hard to increase the ventilation rate. Two scenarios are considered, which are viral contaminants under homogeneous emission in a general room, and viral contaminants emitted from an infector lying in a 6-mat bedroom.

The results showed that a general household HEPA filter air purifier has high effectiveness in removing indoor viral contaminants and infection risks. Specifically in Scenario b, to reach an infection probability of 0.2, it took a susceptible person only about 10 min of exposure time without purifier, but up to 50 min with a purifier.

Higher flow rate contributes to higher overall purifying effectiveness and more thorough air mixing. However, when the flow rate becomes larger, the purifying effectiveness will increase more slowly, and the noise and draft problems may follow if the air purifier is not well-designed.

The purifying efficacy, contaminant concentration distribution, and infection probability distribution is related to the relative positions of the purifier inlet and outlet, ventilation supply and exhaust, virus generation sources, and indoor obstacles such as beds. For example, when the purifier inlet was further away from the ventilation supply, the overall purifying effectiveness would become higher; when the purifier is further away from the virus source, the infection risk will spread more widely.

In addition, if both infector and susceptible person wear a surgical mask, the mean infection probability can be further reduced, and down to almost half of the original under the operation of the air purifier.

On the other hand, this paper only performed a steady-state analysis and neglected the effect of nasal breathing rate on the existing flow and concentration fields in the room, which needs further investigation.

## REFERENCES

Chen, Lin, Xinming Jin, Lijun Yang, Xiaoze Du, and Yongping Yang. 2017. "Particle Transport Characteristics in Indoor Environment with an Air Cleaner: The Effect of Nonuniform Particle Distributions." *Building Simulation* 10 (1): 123–33. https://doi.org/10.1007/s12273-016-0310-7.

Dai, Hui, and Bin Zhao. 2020. "Association of the Infection Probability of COVID-19 with Ventilation Rates in Confined Spaces." *Building Simulation*. https://doi.org/10.1007/s12273-020-0703-5.

F.S. Lien et al. 1996. "Low-Reynolds-Number Eddy-Viscosity Modeling Based on Non-Linear Stress-Strain/Vorticity Relations." In *Proc.3rd Symposium On Engineering Turbulence Modeling and Measurements*.

Fabian, Patricia, James J. McDevitt, Wesley H. DeHaan, Rita O.P. Fung, Benjamin J. Cowling, Kwok Hung Chan, Gabriel M. Leung, and Donald K. Milton. 2008. "Influenza Virus in Human Exhaled Breath: An Observational Study." *PLoS ONE* 3 (7): 5–10. https://doi.org/10.1371/journal.pone.0002691.

Jin, Xinming, Lijun Yang, Xiaoze Du, and Yongping Yang. 2016. "Particle Transport Characteristics in Indoor Environment with an Air Cleaner." *Indoor and Built Environment* 25 (6): 987–96. https://doi.org/10.1177/1420326X15592253.

Konda, Abhiteja, Abhinav Prakash, Gregory A. Moss, Michael Schmoldt, Gregory D. Grant, and Supratik Guha. 2020. "Aerosol Filtration Efficiency of Common Fabrics Used in Respiratory Cloth Masks." *ACS Nano* 14 (5): 6339–47. https://doi.org/10.1021/acsnano.0c03252.

Kowalski, W. J., William P. Bahnfleth, and T. S. Whittam. 1999. "Filtration of Airborne Microorganisms: Modeling and Prediction." *ASHRAE Transactions* 105.

Kriegel, Martin, Udo Buchholz, Petra Gastmeier, Peter Bischoff, Inas Abdelgawad, Anne Hartmann, and Ing Martin Kriegel. 2020. "Predicted Infection Risk for Aerosol Transmission of Sars-Cov-2." *MedRxiv*, 2020.10.08.20209106. https://doi.org/10.1101/2020.10.08.20209106.

Morawska, Lidia, and Junji Cao. 2020. "Airborne Transmission of SARS-CoV-2: The World Should Face the Reality." *Environment International* 139 (April): 105730. https://doi.org/10.1016/j.envint.2020.105730.

Qian, Hua, Yuguo Li, P. V. Nielsen, and Xinhua Huang. 2009. "Spatial Distribution of Infection Risk of SARS Transmission in a Hospital Ward." *Building and Environment* 44 (8): 1651–58. https://doi.org/10.1016/j.buildenv.2008.11.002.

Qian, Hua, Yuguo Li, Hequan Sun, P. V. Nielsen, Xinghua Huang, and Xiaohong Zheng. 2010. "Particle Removal Efficiency of the Portable HEPA Air Cleaner in a Simulated Hospital Ward." *Building Simulation* 3 (3): 215–24. https://doi.org/10.1007/s12273-010-0005-4.

Riley, C.E., Murphy, G. and Riley, R.L. 1978. "Airborne Spread of Measles in a Suburban Elementary School." *American Journal of Epidemiology* 107 (5): 421–32.

Wells, W. F. 1955. *Airborne Contagion and Air Hygiene: An Ecological Study of Droplet Infections*. *Cambridge, MA: Harvard University Press*. Cambridge, MA: Harvard University Press. https://doi.org/10.1093/ajcp/25.11.1301.

Yao, Maosheng, Lu Zhang, Jianxin Ma, and Lian Zhou. 2020. "On Airborne Transmission and Control of SARS-Cov-2." *The Science of the Total Environment* 731: 139178. https://doi.org/10.1016/j.scitotenv.2020.139178.

Zhai, Zhiqiang John, Zhao Zhang, Wei Zhang, and Qingyan Yan Chen. 2007. "Evaluation of Various Turbulence Models in Predicting Airflow and Turbulence in Enclosed Environments by Cfd: Part 1—Summary of Prevalent Turbulence Models." *HVAC and R Research* 13 (6): 853–70. https://doi.org/10.1080/10789669.2007.10391459.

Zhang, Tengfei., Shugang Wang, Gangsen Sun, Linxiao Xu, and Daizo Takaoka. 2010. "Flow Impact of an Air Conditioner to Portable Air Cleaning." *Building and Environment* 45 (9): 2047–56. https://doi.org/10.1016/j.buildenv.2009.11.006.

Zhao, Bin, Yumeng Liu, and Chen Chen. 2020. "Air Purifiers: A Supplementary Measure to Remove Airborne SARS-CoV-2." *Building and Environment* 177 (April): 106918. https://doi.org/10.1016/j.buildenv.2020.106918.

Zhu, Shengwei, Shinsuke Kato, and Jeong-hoon Yang. 2006. "Study on Transport Characteristics of Saliva Droplets Produced by Coughing in a Calm Indoor Environment." *Building and Environment* 41 (12): 1691–1702. https://doi.org/10.1016/j.buildenv.2005.06.024.

Zuraimi, M. S., G. J. Nilsson, and R. J. Magee. 2011. "Removing Indoor Particles Using Portable Air Cleaners: Implications for Residential Infection Transmission." *Building and Environment* 46 (12): 2512–19. https://doi.org/10.1016/j.buildenv.2011.06.008.